

## Bell inequality tests of four-photon six-qubit graph states

Wei-Bo Gao,<sup>1</sup> Xing-Can Yao,<sup>1</sup> Ping Xu,<sup>1</sup> He Lu,<sup>1</sup> Otfried Gühne,<sup>2,3,4</sup> Adán Cabello,<sup>5</sup> Chao-Yang Lu,<sup>1</sup>  
Tao Yang,<sup>1</sup> Zeng-Bing Chen,<sup>1</sup> and Jian-Wei Pan<sup>1,6</sup>

<sup>1</sup>*Department of Modern Physics, Hefei National Laboratory for Physical Sciences at Microscale, University of Science and Technology of China, Hefei, Anhui 230026, China*

<sup>2</sup>*Institut für Quantenoptik und Quanteninformation, Österreichische Akademie der Wissenschaften, Technikerstraße 21A, A-6020 Innsbruck, Austria*

<sup>3</sup>*Institut für Theoretische Physik, Universität Innsbruck, Technikerstraße 25, A-6020 Innsbruck, Austria*

<sup>4</sup>*Fachbereich Physik, Universität Siegen, Walter-Flex-Str. 3, 57068 Siegen, Germany*

<sup>5</sup>*Departamento de Física Aplicada II, Universidad de Sevilla, E-41012 Sevilla, Spain*

<sup>6</sup>*Physikalisches Institut, Ruprecht-Karls-Universität Heidelberg, Philosophenweg 12, D-69120 Heidelberg, Germany*

(Received 25 June 2009; published 27 October 2010)

We now experimentally demonstrate a Y-shaped graph state with photons' polarization and spatial modes as qubits. Based on this state and a linear-type graph state, we report on the experimental realization of two different Bell inequality tests, which represent higher violation than previous Bell tests.

DOI: [10.1103/PhysRevA.82.042334](https://doi.org/10.1103/PhysRevA.82.042334)

PACS number(s): 03.67.Bg, 03.65.Ud, 03.67.Mn, 42.65.Lm

### I. INTRODUCTION

Graph states are basic resources for one-way quantum computation [1], quantum error correction [2], and studying multiparticle entanglement [3]. Moreover, they provide a test bed to investigate quantum nonlocality, that is, the inconsistency between local hidden variable (LHV) theories and quantum mechanics [4–8]. Considerable effort has been devoted to designing different Bell inequalities for graph states with many particles. Here, the aim is to find inequalities with a high quantum mechanical violation, as this is related to the detection efficiency required to perform a loophole-free testing of Bell inequality; moreover, the Bell inequality with a higher violation is more robust against noise. In these studies, it has turned out that, for many kinds of graph states, the violation of local realism increases exponentially with the number of particles [7,8]. Experimental Bell tests with four-qubit cluster or Greenberger-Horne-Zeilinger (GHZ) states, which are examples of graph states, have been reported recently [9–12].

In this paper, we report an experimental realization of Y-shaped graph states  $Y_6$ , which are produced using the polarization and the spatial modes of four photons. Such states are also called hyperentangled states and can be generated with good quality and a high generation rate [11,13–18]. Based on this state and a linear-type one  $LC_6$ , we demonstrate two six-qubit Bell tests, which remarkably represent higher violation than previous experiments on Bell tests. In addition, we give a simple theoretical proof that they give the same high violation of local realism as the six-qubit GHZ state with the Mermin inequality [7], but their violation can be more robust against decoherence in principle.

### II. STATE PREPARATION

Let us first recall the notion of graph states. A graph state  $|G\rangle$  is specified by its stabilizer [3] (i.e., a complete set of operators  $g_i$  of which it is the unique joint eigenstate  $g_i|G\rangle = |G\rangle$  for all  $i$ ), where

$$g_i = X_i \bigotimes_{j \in N(i)} Z_j. \quad (1)$$

Here,  $i$  is some vertex in a graph [see also Fig. 1(a)], and  $N(i)$  denotes its neighborhood, that is, all vertices connected with  $i$ . Furthermore,  $X_i$  and  $Z_j$  denote the usual Pauli operators acting on qubits  $i$  or  $j$ .

In the following, we demonstrate the creation of the desired state. The graph corresponding to the Y-shaped graph state is given in Fig. 1(a) (right), and the experimental setup is shown in Fig. 1(b). First, we use spontaneous parametric down-conversion [19,20] to create one entangled photon pair  $(|H\rangle_1|H\rangle_2 + |V\rangle_1|V\rangle_2)/\sqrt{2}$  and two single photons  $|+\rangle = (|H\rangle + |V\rangle)/\sqrt{2}$ , where  $H, V$  denote horizontal and vertical polarizations, and 1, 2 label the spatial modes of the photons. Earlier, by using operations similar to fusion-II gates between photons [21], we generate a state in

$$|LC_4\rangle = \frac{1}{2}[|H\rangle_1|H\rangle_3(|H\rangle_2|H\rangle_4 + |V\rangle_2|V\rangle_4) + |V\rangle_1|V\rangle_3(|H\rangle_2|H\rangle_4 - |V\rangle_2|V\rangle_4)], \quad (2)$$

which is equivalent to a four-photon linear-type cluster state under local unitary transformations, and here LC refers to the linear-type cluster state [22]. Based on the state  $|LC_4\rangle$ , we apply two Hadamard gates on photons 2 and 4. Then, another two qubits in spatial modes are added to construct the six-qubit state. If a beam of photons enters a polarizing beam splitter (PBS), the  $H$ -polarized one will follow one path, while the  $V$ -polarized one will follow the other path. Here, we define the first path as the photon's  $H'$  spatial mode, and the latter one as its  $V'$  spatial mode. After we place two PBSs in the outputs of photons 1 and 4, the whole state will be converted to

$$\begin{aligned} |Y_6\rangle &= \frac{1}{2}\{|H\rangle_1|H\rangle_3|H\rangle_2|H\rangle_4|H'\rangle_1|H'\rangle_4 \\ &\quad + |H\rangle_1|H\rangle_3|V\rangle_2|V\rangle_4|H'\rangle_1|V'\rangle_4 \\ &\quad + |V\rangle_1|V\rangle_3|H\rangle_2|V\rangle_4|V'\rangle_1|V'\rangle_4 \\ &\quad + |V\rangle_1|V\rangle_3|V\rangle_2|H\rangle_4|V'\rangle_1|H'\rangle_4\} \\ &= \frac{1}{2}\{|0\rangle_1|0\rangle_3|0\rangle_2|0\rangle_4|0\rangle_5|0\rangle_6 \\ &\quad + |0\rangle_1|0\rangle_3|1\rangle_2|1\rangle_4|0\rangle_5|1\rangle_6 + |1\rangle_1|1\rangle_3|0\rangle_2|1\rangle_4|1\rangle_5|1\rangle_6 \\ &\quad + |1\rangle_1|1\rangle_3|1\rangle_2|0\rangle_4|1\rangle_5|0\rangle_6\}. \end{aligned} \quad (3)$$

This is equivalent to a Y-shaped six-qubit graph state up to single-qubit unitary transformations.

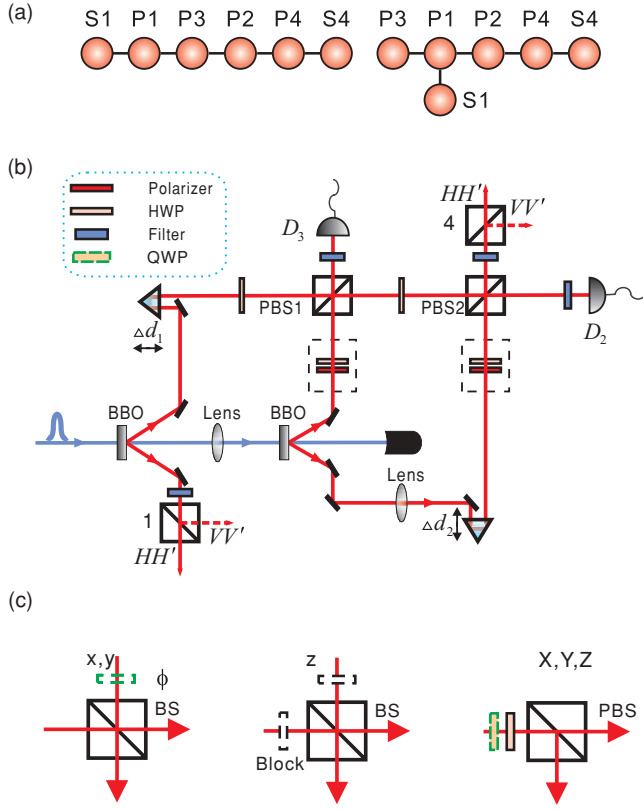


FIG. 1. (Color online) (a) The two graph states created.  $P_i$  represents (polarization) qubit  $i$ , and S1 and S4 represent (spatial) qubits 5 and 6, respectively. (b) Scheme of the experimental setup to generate the desired graph states. Femtosecond laser pulses ( $\approx 200$  fs, 76 MHz, 788 nm) are converted to ultraviolet and are transmitted through two  $\beta$ -barium-borate crystals (2 mm), where two photon pairs are generated. The observed twofold coincident count rate is about  $2.6 \times 10^4$ /s. Two additional polarizers are inserted into the arms of the second pair to prepare two single-photon states. (c) The measurement setups for the desired observables. The first setup is for  $x$  measurement of spatial qubits when  $\phi = 0$ , and for  $y$  measurement of spatial qubits when  $\phi = 90^\circ$ . The second one is for  $z$  measurement of spatial qubits by using blocks in the two paths of the beam splitter (BS). The third one is for  $X, Y, Z$  measurements of polarization qubits by using half-wave plates (HWPs), quarter-wave plates (QWPs), and PBSs.

In the earlier procedure, if we apply two  $\mathcal{H}$  gates on photons 1 and 4 instead of 2 and 4, the state will be a linear-type graph state [23] [see Fig. 1(a) (right)],

$$\begin{aligned}
 |\text{LC}_6\rangle = & \frac{1}{\sqrt{8}} \{ [|0\rangle_5 |0\rangle_1 + |1\rangle_5 |1\rangle_1 ] |0\rangle_3 \otimes [ |\tilde{0}\rangle_2 |0\rangle_4 |0\rangle_6 \\
 & + |\tilde{1}\rangle_2 |1\rangle_4 |1\rangle_6 ] + [|0\rangle_5 |0\rangle_1 - |1\rangle_5 |1\rangle_1 ] |1\rangle_3 \\
 & \otimes [ |\tilde{1}\rangle_2 |0\rangle_4 |0\rangle_6 + |\tilde{0}\rangle_2 |1\rangle_4 |1\rangle_6 ] \}, \quad (4)
 \end{aligned}$$

where  $|\tilde{0}\rangle = (|0\rangle + |1\rangle)/\sqrt{2}$ , and  $|\tilde{1}\rangle = (|0\rangle - |1\rangle)/\sqrt{2}$ .  $|\text{LC}_6\rangle$  is equivalent to a six-qubit linear-type graph state up to single-qubit unitary transformations.

### III. RESULTS OF THE STATE FIDELITY

In order to measure the states' fidelities and to test the Bell inequalities, we need to implement the desired local measurements. The measurement setups are shown in Fig. 1(c), which are similar to Refs. [11,16]. Here, and in the following,  $x, y, z$  refer to the Pauli matrices for the spatial modes, and  $X, Y, Z$  refer to the Pauli matrices of the polarization modes. The measurements of  $x, y$  observables are implemented by overlapping different modes of a photon on a BS, and the measurement of  $z$  observable is implemented by blocking one or the other input path of the BS. The observables of polarization qubits are measured by placing a combination of a QWP, an HWP, and a PBS in front of the single-photon detectors. Although a photon's polarization and spatial information are read out simultaneously, they are independent measurements and have no influence on each other.

The measurements of spatial modes require single-photon interferometers as shown in Fig. 2(a). This interferometer is very easily affected by its environment and can only be stable for a few minutes. In our experiment, an ultrastable Sagnac-ring technique [24,25] is applied to satisfy the required stability. First, we design a crystal combining a PBS and a BS as shown in Fig. 2(c). Then, we construct the single-photon interferometer in a Sagnac-ring configuration [see Fig. 2(b)]. The  $H$ -polarized component is transmitted and propagated through the interferometer in the counterclockwise direction, while the  $V$ -polarized component is reflected and propagated through the interferometer in the clockwise direction. Then, the interference happens when the two components meet at the BS. Such an interferometer can be stable for at least 10 h [18].

To estimate the fidelity of the prepared states, we consider an observable  $B$  with the property  $\langle \phi | B | \phi \rangle \leq \langle \phi | Y_6 \rangle \langle Y_6 | \phi \rangle = F_{Y_6}$  for any  $|\phi\rangle$ . This means  $\langle B \rangle_{\text{expt}}$  is a lower bound of the fidelity of the experimentally produced state [26]. In the experiment, we have chosen the observable  $B$  in Ref. [27] and find  $\langle B \rangle_{\text{expt}} = 0.63 \pm 0.04$ , clearly exceeding  $1/2$  and, thus, proving the genuine six-qubit entanglement of

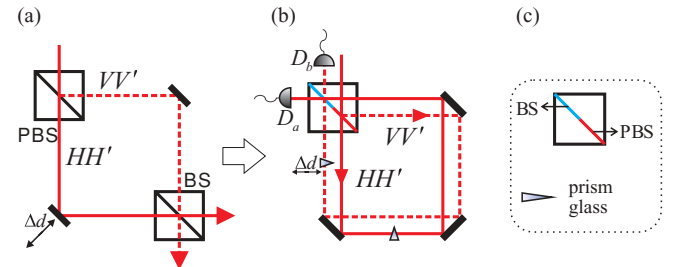


FIG. 2. (Color online) Apparatuses for constructing a Sagnac interferometer in order to measure all the necessary observables of spatial modes. (a) The original scheme of the single-photon interferometer, which is easily affected by the environment and can be stable for only several minutes. (b) Our single-photon interferometer in the Sagnac-ring model. Two special prism glasses are inserted to change optical path delay in order to obtain the desired phase. (c) A special crystal combining the function of BS and PBS.

TABLE I. Experimental values of the observables on  $|LC_6\rangle$  required in the test of the optimal Bell inequality. Each experimental value is obtained by measuring in an average time of 400 s and considers the Poissonian counting statistics of the raw detection events for the experimental errors. The order of the qubits is 5-1-3-2-4-6.

Observable	Value	Observable	Value
$xXZZXx$	$0.61 \pm 0.04$	$-xXZZYy$	$0.60 \pm 0.04$
$xXIYYx$	$0.63 \pm 0.04$	$xXIYXy$	$0.62 \pm 0.04$
$-yYZZXx$	$0.55 \pm 0.04$	$yYZZYy$	$0.56 \pm 0.04$
$-yYIYYx$	$0.65 \pm 0.03$	$-yYIYXy$	$0.56 \pm 0.04$
$xYIIXx$	$0.58 \pm 0.04$	$-xYIYy$	$0.63 \pm 0.04$
$xYXXYx$	$0.58 \pm 0.04$	$xYXXYy$	$0.60 \pm 0.04$
$yXYIXx$	$0.55 \pm 0.04$	$-yXYIYy$	$0.56 \pm 0.04$
$yXXXYx$	$0.57 \pm 0.04$	$yXXXYy$	$0.60 \pm 0.04$

the state [26]. The fidelity of the linear-type graph state is above  $0.61 \pm 0.01$  [23], also proving the genuine six-qubit entanglement.

#### IV. RESULTS OF OPTIMAL BELL INEQUALITIES

The optimal Bell inequality (i.e., the one having the highest resistance to noise) involving only stabilizing observables for the  $LC_6$  state in the form of Eq. (4) is

$$\langle \mathcal{B}_{LC_6} \rangle = \langle (\mathbb{1} + g_5)g_1(\mathbb{1} + g_3)(\mathbb{1} + g_2)g_4(\mathbb{1} + g_6) \rangle \leq 4, \quad (5)$$

where  $g_5 = z_5Z_1$ ,  $g_1 = x_5X_1Z_3$ ,  $g_3 = Z_1X_3Z_2$ ,  $g_2 = Z_3X_2Z_4$ ,  $g_4 = Z_2X_4x_6$ , and  $g_6 = Z_4z_6$  [6]. These  $g_i$  are stabilizing operators of the linear-type graph state (i.e., the graph state is an eigenstate of all the  $g_i$  with eigenvalue +1), as one can easily check. This writing of the Bell operator is only a shorthand notation, and the required measurements for the Bell test are the ones that arise *after* multiplying out  $\mathcal{B}_{LC_6}$  (see Table I). As all the terms in the Bell operator are products of stabilizing operators, the cluster state is an eigenstate of all these terms, and the value for the ideal cluster state is the algebraic maximum  $\langle \mathcal{B}_{LC_6} \rangle = 16$ .

TABLE II. Experimental values of all the observables on  $|Y_6\rangle$  for the optimal Bell inequality measurement. Each experimental value is obtained by measuring in an average time of 400 s, and propagated Poissonian statistics of the raw detection events are also considered. The order of the qubits is 1-3-2-4-5-6.

Observable	Value	Observable	Value
$-XXIYxy$	$0.62 \pm 0.04$	$XYIYyy$	$0.59 \pm 0.05$
$YYIYxy$	$0.58 \pm 0.05$	$YXIYyy$	$0.61 \pm 0.05$
$XXIXxx$	$0.56 \pm 0.04$	$-XYIXyx$	$0.54 \pm 0.04$
$-YYIXxx$	$0.61 \pm 0.04$	$-YXIXyx$	$0.63 \pm 0.04$
$-YXZXxy$	$0.57 \pm 0.05$	$YYZXyy$	$0.62 \pm 0.04$
$-XYZXxy$	$0.55 \pm 0.04$	$-XXZXyy$	$0.58 \pm 0.04$
$-YXZYxx$	$0.54 \pm 0.04$	$YYZYyx$	$0.57 \pm 0.05$
$-XYZYxx$	$0.59 \pm 0.04$	$-XXZYyx$	$0.54 \pm 0.04$

Similarly, the optimal stabilizer Bell inequality for the  $Y_6$  state is [6]

$$\langle \mathcal{B}_{Y_6} \rangle = \langle (\mathbb{1} + g_3)g_1(\mathbb{1} + g_5)(\mathbb{1} + g_2)g_4(\mathbb{1} + g_6) \rangle \leq 4, \quad (6)$$

where now  $g_3 = Z_1Z_3$ ,  $g_1 = X_1X_3X_2x_5$ ,  $g_5 = Z_1z_5$ ,  $g_2 = Z_1Z_2Z_4$ ,  $g_4 = Z_2Z_4z_6$ , and  $g_6 = Z_4z_6$ . Again, the value for the pure  $Y_6$  state is  $\langle \mathcal{B}_{Y_6} \rangle = 16$ .

A remarkable feature of these Bell inequalities is that the  $LC_6$  state and the  $Y_6$  state violate local realism by a factor of 4, which is also the violation for the six-qubit GHZ state, if only stabilizing elements are considered (the optimal Bell inequality is then the Mermin inequality [6]). However, the  $LC_6$  and  $Y_6$  states are more resistant to decoherence than the  $GHZ_6$  state [28]. In fact, one can directly see that if decoherence acts as a depolarizing channel on each qubit, the violation of the Mermin inequality for the  $GHZ_6$  state decreases faster than for the graph states considered here. Namely, if noise such as  $\rho \mapsto p\rho + (1-p)\mathbb{1}/2$  is acting on each qubit separately, the value of the Mermin inequality decreases with  $p^6$ , as the Mermin inequality consists only of full correlation terms. In our Bell inequalities, however, half of the terms contain the identity on one qubit (see Tables I and II), which means that they decay only with  $p^5$ , and the total violation decreases such as  $(p^6 + p^5)/2$ . This proves that the nonlocality vs decoherence ratio of GHZ states is not universal: There are states with a similar violation, which are more robust against decoherence.

The experimental results are given in Tables I and II. From these data, we find

$$\begin{aligned} \langle \mathcal{B}_{LC_6} \rangle_{\text{expt}} &= 9.40 \pm 0.16, \\ \langle \mathcal{B}_{Y_6} \rangle_{\text{expt}} &= 9.30 \pm 0.17, \end{aligned} \quad (7)$$

which violate the classical bound by 34 and 31 standard deviations.

Let us consider the ratio  $\mathcal{D}$  between the quantum value of the Bell operator and its bound in LHV theories. Experimentally, we have

$$\begin{aligned} \mathcal{D}_{LC_6} &= \langle \mathcal{B}_{LC_6} \rangle_{\text{expt}} / \langle \mathcal{B}_{LC_6} \rangle_{\text{LHV}} = 2.35 \pm 0.04, \\ \mathcal{D}_{Y_6} &= \langle \mathcal{B}_{Y_6} \rangle_{\text{expt}} / \langle \mathcal{B}_{Y_6} \rangle_{\text{LHV}} = 2.33 \pm 0.04. \end{aligned} \quad (8)$$

These are larger values compared to previous experiments with similar Bell inequalities for four-qubit cluster states: There, values of  $\mathcal{D}$  from 1.29 to 1.70 have been achieved [9–11]; using a Bell inequality with nonstabilizer observables for the four-qubit GHZ state,  $\mathcal{D} = 2.22$  has been reached [12]. To our knowledge, these were the best values obtained so far. Therefore, despite having a lower fidelity than in the four-qubit experiments, we find a higher violation of local realism, which demonstrates that the amount of nonlocality can increase with the number of qubits. This might help in designing loophole-free Bell inequality tests [29].

We would like to add that the generation of the graph states and the observation of the Bell inequality violations using hyperentanglement implies that some of the qubits are carried by the same photon, and, therefore cannot, be spatially separated. So our setup cannot be used to close the locality loophole. However, as the measurements on the polarization

qubit and the spatial qubit are independent, such experiments can be viewed as a test of the Kochen-Specker theorem [30,31] in order to refute noncontextual hidden variable models.

## V. CONCLUSION

We have created a Y-shaped four-photon six-qubit graph state entangled in the photons' polarization and spatial modes and proved its genuine six-qubit entanglement. Furthermore, we have implemented two multiqubit Bell tests based on them, which show the highest violation of Bell inequality so far. It is interesting to investigate the relationship between decoherence

and nonlocality further. The aim is to characterize states, which show a high violation of local realism, while still being robust against decoherence.

## ACKNOWLEDGMENTS

This work is supported by the NNSF of China, the CAS, and the National Fundamental Research Program (under Grant No. 2006CB921900). O.G. acknowledges support from the FWF (START prize) and the EU (OLAQUI, SCALA, and QICS). A.C. acknowledges support by the Projects No. P06-FQM-02243 and No. FIS2008-05596.

- 
- [1] R. Raussendorf and H. J. Briegel, *Phys. Rev. Lett.* **86**, 5188 (2001); M. Van den Nest, A. Miyake, W. Dür, and H. J. Briegel, *ibid.* **97**, 150504 (2006).
- [2] D. Schlingemann and R. F. Werner, *Phys. Rev. A* **65**, 012308 (2001); D. Schlingemann, *Quantum Inf. Comput.* **2**, 307 (2002).
- [3] M. Hein, J. Eisert, and H. J. Briegel, *Phys. Rev. A* **69**, 062311 (2004); M. Hein *et al.*, in *Quantum Computers, Algorithms and Chaos*, edited by G. Casati, D. L. Shepelyansky, P. Zoller, and G. Benenti (IOS, Amsterdam, 2006).
- [4] V. Scarani, A. Acin, E. Schneck, and M. Aspelmeyer, *Phys. Rev. A* **71**, 042325 (2005); J. Barrett, C. M. Caves, B. Eastin, M. B. Elliott, and S. Pironio, *ibid.* **75**, 012103 (2007); O. Gühne and A. Cabello, *ibid.* **77**, 032108 (2008).
- [5] A. Cabello and P. Moreno, *Phys. Rev. Lett.* **99**, 220402 (2007).
- [6] A. Cabello, O. Gühne, and D. Rodríguez, *Phys. Rev. A* **77**, 062106 (2008).
- [7] N. D. Mermin, *Phys. Rev. Lett.* **65**, 1838 (1990).
- [8] O. Gühne, G. Tóth, P. Hyllus, and H. J. Briegel, *Phys. Rev. Lett.* **95**, 120405 (2005); G. Tóth, O. Gühne, and H. J. Briegel, *Phys. Rev. A* **73**, 022303 (2006); L.-Y. Hsu, *ibid.* **73**, 042308 (2006).
- [9] P. Walther, M. Aspelmeyer, K. J. Resch, and A. Zeilinger, *Phys. Rev. Lett.* **95**, 020403 (2005).
- [10] N. Kiesel, C. Schmid, U. Weber, G. Tóth, O. Gühne, R. Ursin, and H. Weinfurter, *Phys. Rev. Lett.* **95**, 210502 (2005).
- [11] G. Vallone, E. Pomarico, P. Mataloni, F. De Martini, and V. Berardi, *Phys. Rev. Lett.* **98**, 180502 (2007).
- [12] Z. Zhao, T. Yang, Y.-A. Chen, A.-N. Zhang, M. Żukowski, and J.-W. Pan, *Phys. Rev. Lett.* **91**, 180401 (2003).
- [13] P. G. Kwiat, *J. Mod. Opt.* **44**, 2173 (1997).
- [14] J. T. Barreiro, N. K. Langford, N. A. Peters, and P. G. Kwiat, *Phys. Rev. Lett.* **95**, 260501 (2005).
- [15] G. Vallone, E. Pomarico, F. De Martini, and P. Mataloni, *Phys. Rev. Lett.* **100**, 160502 (2008).
- [16] K. Chen, C.-M. Li, Q. Zhang, Y.-A. Chen, A. Goebel, S. Chen, A. Mair, and J.-W. Pan, *Phys. Rev. Lett.* **99**, 120503 (2007).
- [17] H. S. Park *et al.*, *Opt. Express* **15**, 17960 (2007).
- [18] W.-B. Gao *et al.*, *Nat. Phys.* **6**, 331 (2010).
- [19] P. G. Kwiat, K. Mattle, H. Weinfurter, A. Zeilinger, A. V. Sergienko, and Y. Shih, *Phys. Rev. Lett.* **75**, 4337 (1995).
- [20] Z. Zhao *et al.*, *Nature (London)* **430**, 54 (2004).
- [21] D. E. Browne and T. Rudolph, *Phys. Rev. Lett.* **95**, 010501 (2005).
- [22] Y. Tokunaga, S. Kuwashiro, T. Yamamoto, M. Koashi, and N. Imoto, *Phys. Rev. Lett.* **100**, 210501 (2008).
- [23] W.-B. Gao, P. Xu, X.-C. Yao, O. Gühne, A. Cabello, C.-Y. Lu, C.-Z. Peng, Z.-B. Chen, and J.-W. Pan, *Phys. Rev. Lett.* **104**, 020501 (2010).
- [24] T. Nagata *et al.*, *Science* **316**, 726 (2007).
- [25] M. P. Almeida *et al.*, *Science* **316**, 579 (2007).
- [26] O. Gühne and G. Tóth, *Phys. Rep.* **474**, 1 (2009).
- [27] See the online material of C.-Y. Lu, W.-B. Gao, O. Gühne, X.-Q. Zhou, Z.-B. Chen, and J.-W. Pan, *Phys. Rev. Lett.* **102**, 030502 (2009).
- [28] W. Dür and H.-J. Briegel, *Phys. Rev. Lett.* **92**, 180403 (2004).
- [29] A. Cabello, D. Rodríguez, and I. Villanueva, *Phys. Rev. Lett.* **101**, 120402 (2008).
- [30] G. Kirchmair *et al.*, *Nature (London)* **460**, 494 (2009).
- [31] E. Amselem, M. Rådmark, M. Bourennane, and A. Cabello, *Phys. Rev. Lett.* **103**, 160405 (2009).